Comparing Downlink Capacity between Super Wi-Fi and Wi-Fi in Multi-Floored Indoor Environments

Gyumin Hwang

Department of Electrical Engineering
Graduate school of UNIST

Comparing Downlink Capacity between Super Wi-Fi and Wi-Fi in Multi-Floored Indoor Environments

Gyumin Hwang

This certifies that the thesis of Gyumin Hwang is approved.

1. 27. 2014

Signature

Thesis Supervisor: Hyoil Kim

Signature

Changhee Joo: Thesis Committee Member #1

Signature

Hyun Jong Yang: Thesis Committee Member #2

Comparing Downlink Capacity between Super Wi-Fi and Wi-Fi in Multi-Floored Indoor Environments

A thesis
submitted to the Graduate School of UNIST
in partial fulfillment of the
requirements for the degree of
Master of Science

Gyumin Hwang

1. 27. 2014
Approved by

Major Advisor
Hyoil Kim

Abstract

Super Wi-Fi is a Wi-Fi-like service exploiting TV white spaces (WS) via the cognitive radio technology which is expected to achieve larger coverage than today's Wi-Fi thanks to its superior propagation characteristics. Super Wi-Fi is currently being materialized as an international standard, IEEE 802.11af, targetting indoor and outdoor applications. This thesis demonstrates the potential of Super Wi-Fi in indoor environments by measuring its signal propagation characteristics and comparing them with those of Wi-Fi in the same indoor structure. Specifically, this thesis measures the wall and floor attenuation factors and path-loss distribution in 770 MHz and 2.4 GHz, and estimates the downlink capacity of Super Wi-Fi and Wi-Fi according to wide-accepted indoor path loss models. The experimental results reveal that TVWS signals can penetrate up to two floors and provide favorable coverage up to one floor above and below. In addition, TVWS can not only extend the coverage of Wi-Fi but also significantly mitigate shaded regions of Wi-Fi while achieving almost homogeneous data rates in the Wi-Fi's coverage. The observed phenomena imply that Super Wi-Fi may be suitable for indoor applications with requirements of low-to-moderate data rates, extended horizontal and vertical coverage, and fair rate distribution within the service coverage.

Contents

List of Figures

List of Tables

Nomenclature

CR	Cognitive Radio
UHD	USRP Hardware Driver
DTV	Digital TV
FAF	Floor Attenuation Factor
ISM	Industrial, Scientific and Medical
TVWS	TV White Space
Rx	Receiver
SDR	Software Defined Radio
SNR	Signal-to-Noise-Ratio
Tx	Transmitter
UHF	Ultra High Frequency
USRP	Universal Software Radio Peripheral
U-NII	Unlicensed National Information Instructure
VHF	Very High Frequency
WAF	Wall Attenuation Factor

Chapter 1

Introduction

In the past few decades, there has been a tremendous amount of incease in the number of wireless devices including laptops, smart phones, and tablets. Such growth in wireless usage leads to the ever-increasing demand to more spectrum, which is expected to cause spectrum scarcity in the near future due to the limited spectrum resources with fair characteristics. However, it has been revealed that spectrum scarcity is rooted at inefficient spectrum utilization as shown in Figure 1.1 [1] which is regarding the usage pattern of spectrum resources in Washington DC during one month. As seen, most spectrum usage is concentrated at certain spectrum bands, leaving others severely under-utilized.

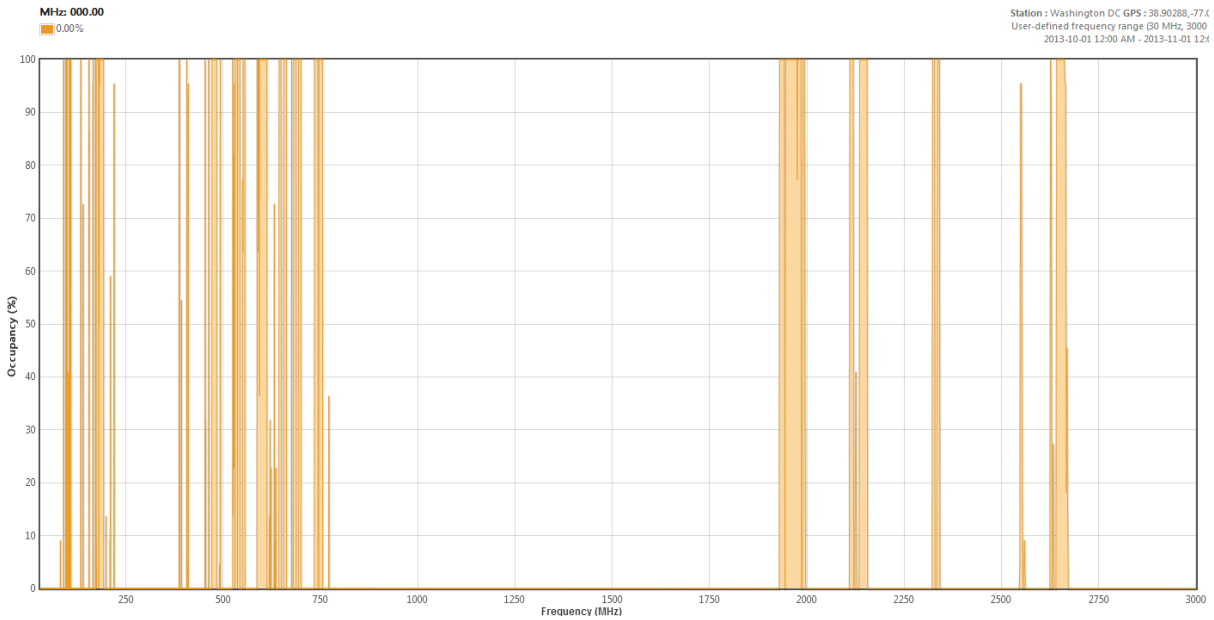

Figure 1.1: Frequcny resource using pattern [1].

Cognitive radio (CR) is a promising technology that may resolve the spectrum scarcity by enhancing the spectrum utilization. To utilize the spectrum, a CR device monitors spectrum bands and determines which bands are temporarily unused by their incumbent users. The identified idle bands are utilized by unlicensed CR users only when they are free of incumbent users, for which the CR users keep monitoring

the bands and evict them immediately at the return of the incumbents. Such behavior of CR devices has been made possible thanks to the reprogrammable software defined radio (SDR) based design.

There exist some CR related standards, where IEEE 802.22 and IEEE 802.11af are two representative standards with different service scenarios – IEEE 802.22 is a wireless regional area network (WRAN) standard aiming at serving the wireless Internet with up to 100 km coverage, while IEEE 802.11af builds upon the 802.11ac WLAN standard aiming at serving the wireless Internet with up to 5 km coverage which is often called Super Wi-Fi.

Super Wi-Fi is a TV White Space (TVWS)-based Wi-Fi service, which is similar to Wi-Fi. Wi-Fi freely uses the industrial, scientific and medical (ISM) bands (2.4 GHz) and unlicensed national information instructure (U-NII) bands (5 GHz) without any approval whereas Super Wi-Fi has to identify an temporarily-idle channel in TVWS by using the CR technology to utilize the spectrum. TVWS refers to unused frequency band of very high frequency (VHF) and ultra high frequency (UHF) which are allocated for TV broadcasting, and this band is 54-698MHz in US and Korea. The FCC approved that unlicensed user who observes the regulation uses TVWS as non-licensed band. Especially, the switchover from analog television to digital television was an opportunity to extend its white space (WS) in TV frequency band because digital transmission can transmit the same amount data using fewer channels than analog transmission.

Super Wi-Fi has the superior frequency characteristics such as penetrability and path loss because it is utilizing VHF and UHF bands that lie in much lower spectrum than ISM and U-NII. That is, Super Wi-Fi is expected to be able to cover the same area with less power than Wi-Fi. In addition, it makes it easier to manage the network and mitigates existing problems of Wi-Fi such as shaded areas and the airtime fairness problem [2]. In particular, stations in Wi-Fi service area have dramatically different data rates depending on their locations since Wi-Fi signals lose significant energy as they travel through obstacles and uneven terrain. For example, Figure 1.2 [3] shows an example when nodes 1, 2 and 3 communicate at 11 Mbps with each other and the data rate R between nodes 4 and 5 is varied from 11 Mbps to 1 Mbps, the throughput of link 2-3 and link 4-5 are decreased because the link 4-5 occupies more time as the data rate R is decreased.

In this thesis, we demonstrate the benefit of deploying Super Wi-Fi indoors by identifying its superior characteristics to Wi-Fi via experimental studies. Although there exist various work modeling the indoor signal propagation either at VHF/UHF bands [4, 5, 6, 7, 8] or at ISM/UNII bands, there have been no result that compares the propagation characteristics of the two bands in the same indoor environment.

The contribution of this thesis is three-fold. First, we performed an extensive measurement study that compares the signal propagation characteristics of Super Wi-Fi and Wi-Fi in the same indoor environment, including wall and floor attenuation factors and path-loss exponents. Second, we demonstrate

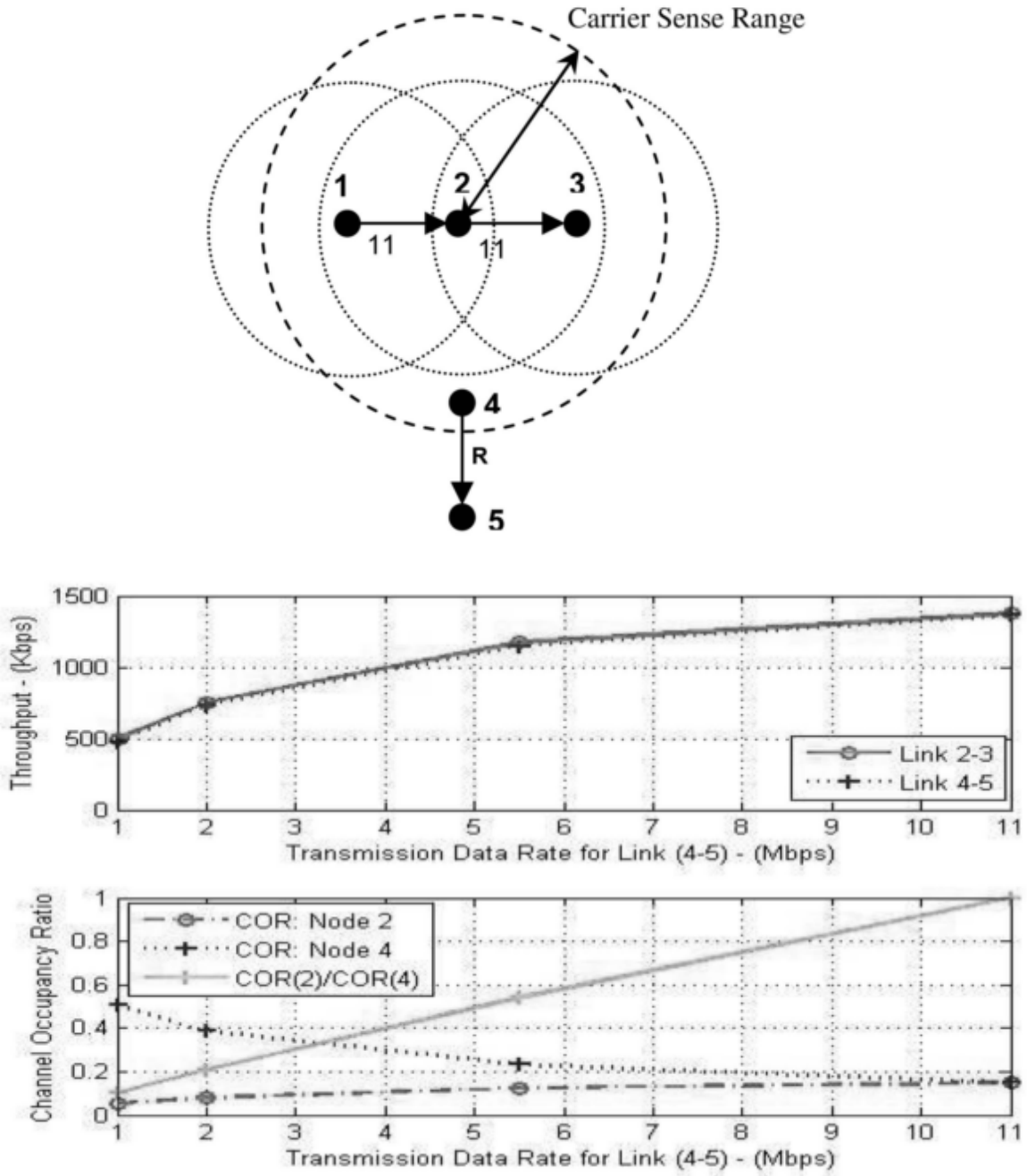

Figure 1.2: Example of airtime fairness problem.

the efficacy of exploiting TVWS for future indoor Wi-Fi applications such as extended coverage and near-homogeneous achievable data rates. Lastly, we predict the coverage and average capacity of an indoor Super Wi-Fi network by applying the experimental data to a path-loss model.

The rest of the thesis is organized as follows. Section 2 reviews related work, and Sections 3.1, 3.2 and 3.3 explain background knowledge about USRP, GNU Radio and path loss prediction models. Sections 4.1 and 4.2 present the experimental setup. Sections 5.1 and 5.2 investigate the wall and floor attenuation factors of TVWS and UNII bands, and Sections 5.3 and 5.4 describe the location-specific signal-to-noise ratio (SNR) in the indoor environment and estimates average downlink capacity of Super Wi-Fi and Wi-Fi. Finally, the thesis concludes with Section 6.

Chapter 2

Related Work

The indoor signal propagation has been characterized in many studies via field measurements in VHF, UHF, and ISM bands. Zvanovec et al. [9] measured a received signal strength in 2.4 GHz and compared it with a predicted received signal strength obtained from Multi-Wall propagation predict model. Anderson and Rappaport [10] measured a path loss and derived a path loss exponent from measurement in 2.5 and 60 GHz. Andrusenko et al. [11] conducted a path loss measurement in 30, 49 and 87.5 MHz. Seidel and Rappaport [8] measured path loss in four types of buildings. Honcharenko et al. [5] also measured path loss in office building. Gajewski et al. [12] conducted a floor attenuation factor measurement in 30, 49 and 87.5 MHz, and verified the General Urban Path Loss (GUPL) model published in [11] Taylor et al. [13] measured a wall attenuation over 100 MHz to 3 GHz frequency range. Pena et al. [14] also conducted a wall attenuation measurement in 900 MHz band. Nevertheless, none of them compared the characteristics of TVWS and ISM bands in the same indoor environment.

Although Simic et al. [15] have compared indoor signal propagation of TVWS (630 MHz) and ISM (2.4 GHz), their results are analytical predictions by a log-distance path loss model which are not based on real measurements.

Chapter 3

Preliminaries

3.1 USRP

The Universal Software Radio Peripheral (USRP) is a software defined radio device created by Ettus Research and used in both academia and industry to implement a radio system, and there are several versions of USRP such as USRP Networked, Bus and Embedded series [16]. The USRP consists of a mother board and a replaceable daughter board, where the daughter board modulates the baseband signal obtained from the mother board to tune into a target frequency band. The mother board is connected to a host PC through USB 2.0 or Gigabit Ethernet, provides clock for timing, and sends/receives baseband samples to/from the host PC. To control the USRP, the USRP Hardware Driver (UHD) is needed, and it works on various platforms such as Linux, Windows and Mac. Users are able to use the UHD sofrware standalone or with third-party applications like GNU Radio, MATLAB, Simulink, and LabVIEW, to control the USRP and implement software radio systems. Figure 3.1 shows the block digram of a USRP structure.

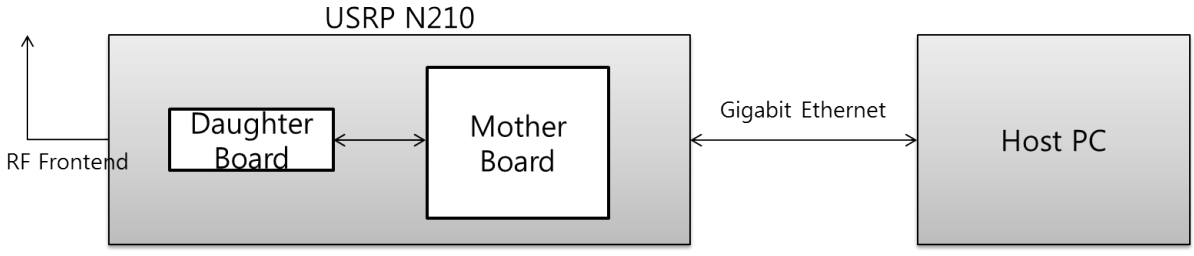

Figure 3.1: Block diagram of USRP N210

The USRP's transmission power is controlled by two variables – *gain* and *amp*. The gain implies the analog gain at the power amplifier, and the amp represents the digital amplitude of the signal samples. Controlling transmission power is an important issue since unsuitably chosen gain and amp make trans-

mission power dispersed out of the signal bandwidth thus resulting in incorrect SNR due to the increase noise floor. Such a phenomenon is called out-of-band signal emission which is believed to be caused by signal amplitude saturation at the analog power amplifier. Figure 3.2 illustrates the impact of gain and amp. In the upper figure, the signal is a trapezoidal shape which can be easily detected and decoded at a receiver. In the lower figure, however, the signal and noise have similar power thus making the receiver hard to decode the signal. More details on the issue will be explained later in section 5.4.

USRP N210 is one of the USRP Networked series that provides 100 MS/s dual ADC and 400 MS/s dual DAC. USRP N210 connects itself with a host PC through Gigabit Ethernet, which supports the communication speed between the USRP and the host PC up to 50 MS/s. This kind of connection method is much faster than older USRPs (e.g., USRP1) which connect themselves to a host PC through USB 2.0 with up to 8 MS/s. USRP N210 also offers MIMO capability via a MIMO cable combining two USRPs together.

3.2 GNU Radio

GNU Radio is a free and open-source development tool kit that provides signal processing blocks to implement software radios [17]. Users can implement a software radio system by using GNU Radio libraries and RF devices like USRP instead of expensive hardware radio systems, or by using GNU Radio alone. The GNU Radio library consists of DSP blocks where they are wrriten in C++ to enhance their performance. For flexible and convenient interface, SWIG wraps the blocks in Python, and users can write a flow-graph (application) by creating and connecting blocks. Figure 3.3 shows the example of a wide band FM receiver flow-graph.

GNU Radio also supports GUI-based development, called GNU Companion, with which user can write a flow-graph by simply dragging and dropping blocks. Figure 3.4 shows a realization of the wide band FM receiver in Figure 3.3.

3.3 Path Loss Prediction Model

In general, predicting path loss is a complicated task due to the random effect from the surrounding environments such as multipath fading. To enhance the accuracy of prediction, there have been various methods proposed. First, deterministic methods such as ray-tracing predict path loss according to the physical law of wave propagation. Although the deterministic methods are usually quite accurate, they need detailed information on the obstacles in the path of signal propagation and require a large amount of time calculating the path loss. On the other hand, statistical methods such as Okumura-Hata [18],

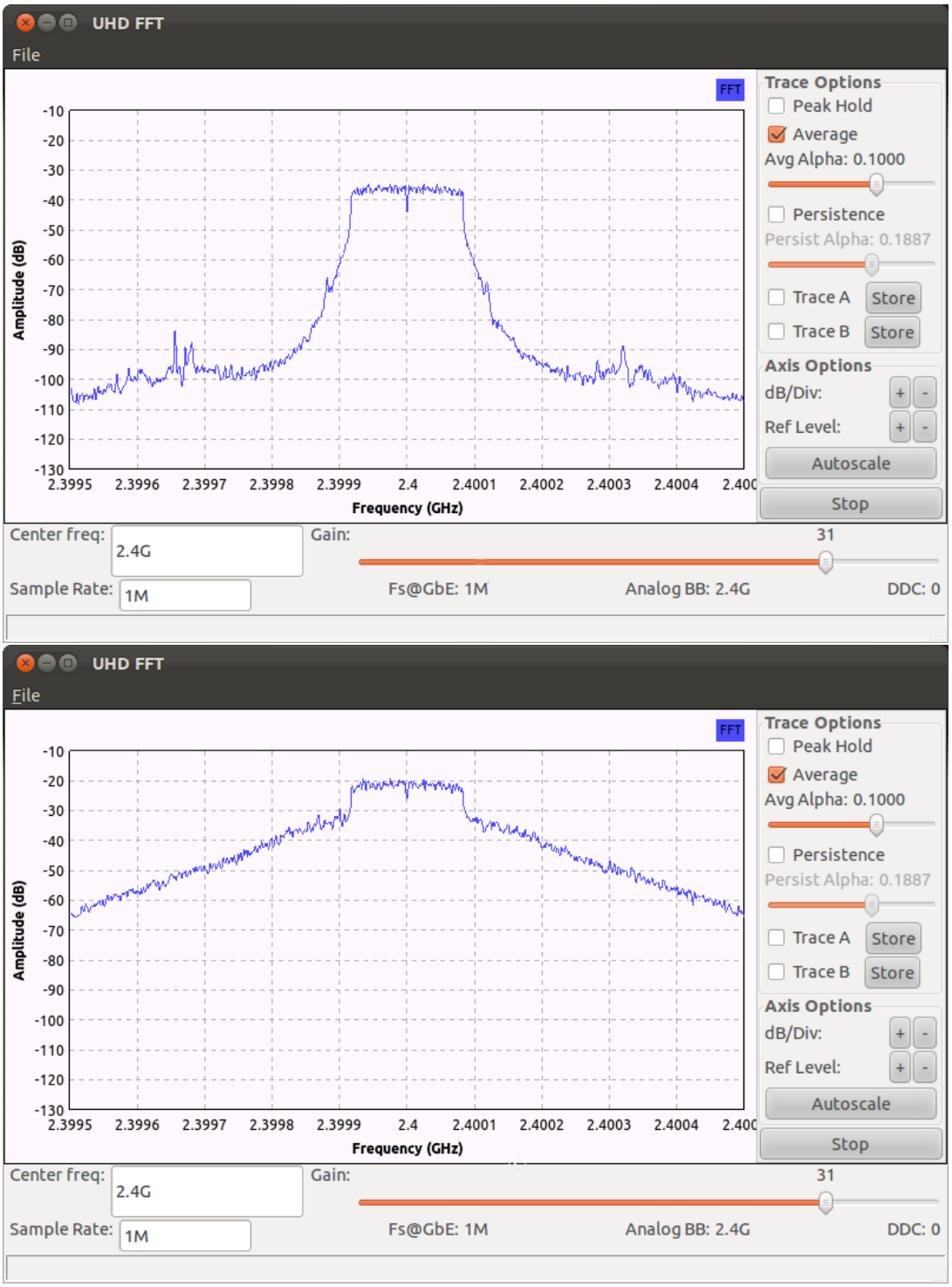

Figure 3.2: Example of controlling USRP transmission power

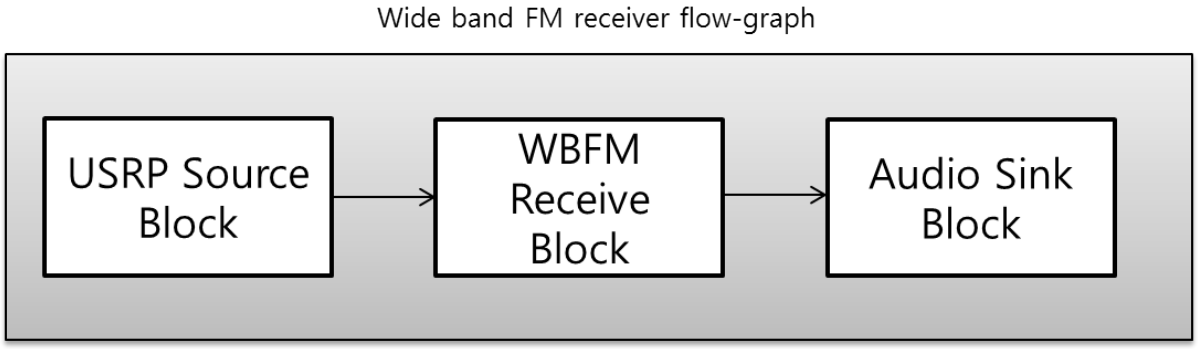

Figure 3.3: Blocks of wide band FM receiver

COST 231 model [19], and GUPL model [11] utilize measured and averaged loss in several typical propagation scenarios. The statistical methods usually yield less accurate results than the deterministic ones. They, however, spend less time calculating the path loss and work with limited information.

It is especially hard to predict path loss in indoor environments because there are many obstacles such as walls, doors and partitions. Therefore, there have been many prediction models proposed in the literature as introduced in the following. The log-distance path loss model [20] predicts path loss by considering the distance between a transmitter and a receiver such that

$$PL(dB) = PL(d_0) + 10n \cdot log(\frac{d}{d_0}) + X_\sigma \tag{3.1}$$

where $PL(dB)$ is the total path loss in dB, $PL(d_0)$ is the path loss in dB at the reference distance d_0, d is the distance between the transmitter and the receiver, and X_σ is a Gaussian random variable with zero mean which reflects the attenuation by fading.

The attenuation factor models [20] consider site-specific obstacles such as partitions and floors which may cause significant path loss. Among those, the floor attenuation factor (FAF) path loss model [8] considers the path loss in a multi-floored building such that

$$\overline{PL}(d)[dB] = \overline{PL}(d_0)[dB] + 10n_{SF} \cdot log(\frac{d}{d_0}) + FAF[dB] \tag{3.2}$$

where $\overline{PL}(d)[dB]$ is the average path loss in dB, $\overline{PL}(d_0)[dB]$ is the path loss at the reference distance d_0, n_{SF} represents the same floor path loss exponent, and FAF represents the floor attenuation factor.

On the other hand, the Multi-Wall Model [21] considers both wall attenuation factor (WAF) and FAF, such that

$$L_{MW} = L_{FSL}(d) + \sum_{i=1}^{N} k_{wi} L_{wi} + k_f L_f \tag{3.3}$$

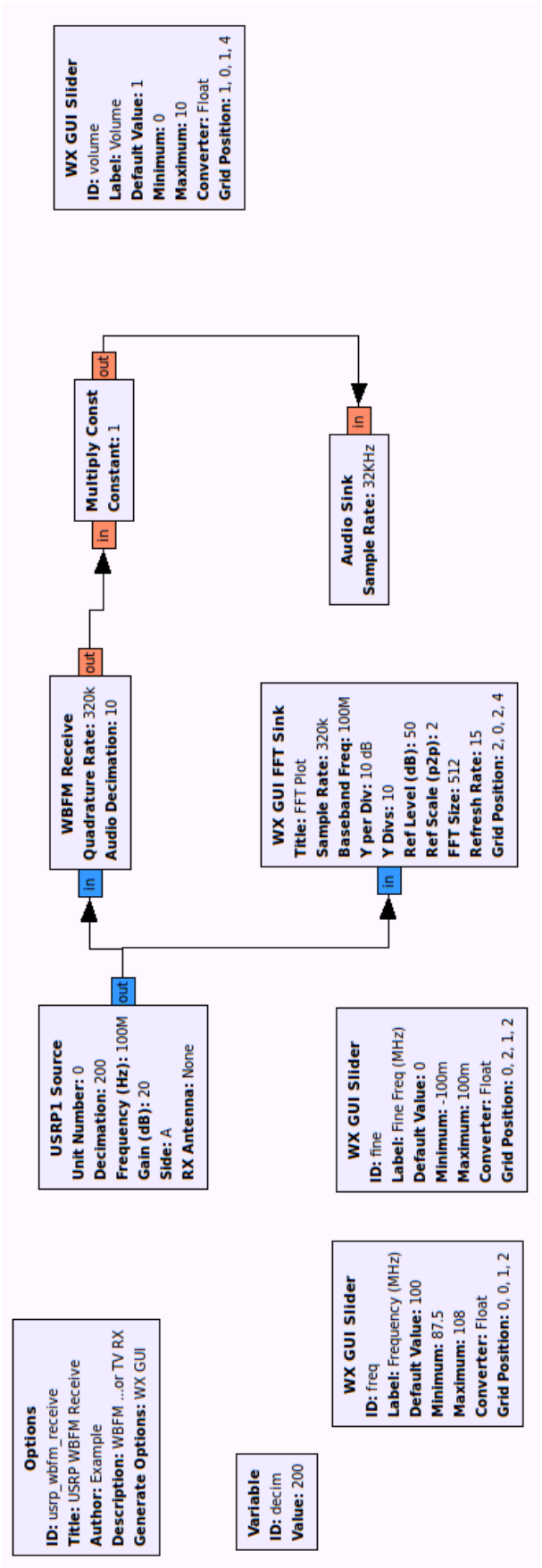

Figure 3.4: Example of GNU Radio Companion

where L_{MW} is the path loss between a transmitter and a receiver in dB, L_{FSL} is the free space path loss at the distance of d meters in dB, N is the number of wall types, k_{wi} is the number of i-th walls, L_{wi} represents wall attenuation factor for i-th type wall, k_f is the number of floors, and L_f is the floor attenuation factor.

The ITU indoor path loss model [22] is intended to predict the path loss between a tranmitter and a receiver in indoor environments and doesn't consider the wall attenuation factor. Its basic form is given as

$$L_{total} = 20log_{10}f + N \cdot log_{10}d + L_f(n) - 28 \tag{3.4}$$

where L is the total loss, N represents the distance power loss coefficient, f is frequency, d is the distance in meters between the transmitter and the receiver, L_f is the floor attenuation loss in dB, and n is the number of floors between the transmitter and the receiver. Typical parameters based on various measurement results are given in Tables 3.1 and 3.2 [22].

These attenuation factor models draw a straight line between the transmitter and the receiver and considers the number of floors and walls that the straight line encounters. This is called primary ray tracing, and it has been shown that the primary ray tracing model predicts path loss quite accurately if properly-chosen path loss exponents, FAF and WAF are used.

Frequency	Residential	Office	Commercial
900 MHz	-	33	20
1.2 - 1.3 GHz	-	32	22
1.8 - 2 GHz	28	30	22
4 GHz	-	28	22
5.2 GHz	-	31	-
60 GHz	-	22	17

Table 3.1: Power loss coefficients, N, for indoor environments

Frequency	Residential	Office	Commercial
900 MHz	-	9 (1 floor) 19 (2 floors) 24 (3 floors)	-
1.8 - 2 GHz	$4n$	15 + $4(n-1)$	6 + $3(n-1)$
5.2 GHz	-	16 (1 floor)	-

Table 3.2: Floor attenuation factors, L_f(dB)

Chapter 4

Experimental Setup

The following sections describe the measurement setup for the wall attenuation factor (WAF), the floor attenuation factor (FAF) and path loss measurements.

4.1 Frequency & Antenna

TVWS in Korea lies on 54-698 MHz (ch 2-51), and Figure 4.1 [23] shows TVWS in Korea and the distribution of DTV channels. Subject to the Radio Regulation Law in Korea, we conduct our experiments with 200 kHz bandwidth centered at 770 MHz frequency. Although this does not exactly match a TVWS band, it is one of the closest frequency to TVWS allowed for experimental purpose in Korea. Other candidate frequencies includ 1134 and 1197 MHz with 650 kHz, and lower frequencies with much narrower bandwidth. Although the chosen band has a limited bandwidth of 200 kHz which is much narrower than the bandwidth of Super Wi-Fi and Wi-Fi (6-8 MHz and 20 MHz respectively), it is free of wireless microphones that coexist in some parts of TVWS in Korea. As a result, there are no interference in the 770 MHz in principle which has been also comfirmed by our measurements.

Wi-Fi lies over the industrial, scientific and medical (ISM) radio bands and the Unlicensed National Information Infrastructure (U-NII) radio bands. To represent Wi-Fi, 2.401 GHz frequency band was

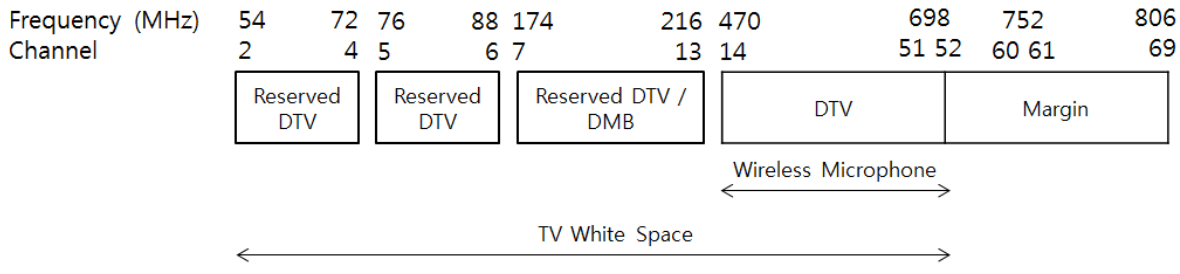

Figure 4.1: TVWS in Korea

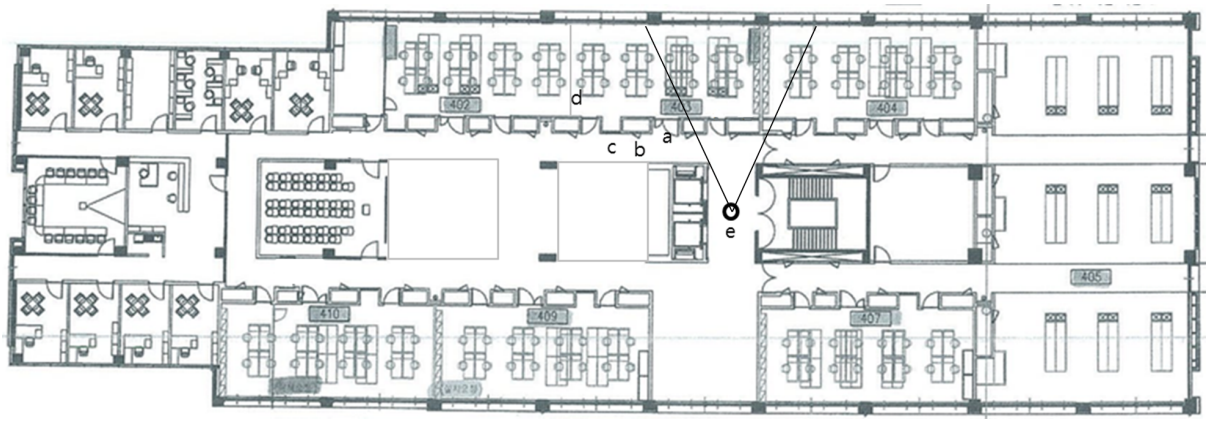

Figure 4.2: Floor plan of the EB2 building of UNIST

selected which is within the ISM bands, because (i) the U-NII radio band suffers from more severe path loss than ISM, and (ii) 2.401 GHz is in the gurad band of Wi-Fi channels so there exist no interfering APs. Our measurements reveal that the level of interference from the Wi-Fi devices in the adjacent bands is not substantial.

4.2 Locations and HW/SW Setup

All measurements were conducted on the third, fourth and fifth floors of the EB2 building of UNIST, South Korea. The building was constructed in 2010 and consists of steel reinforced concrete with constructed marble floors, metal doors, and concrete and ply wood walls. The building has two staircases, two elevators, and several utility rooms at the center of the building structure. Figure 4.2 shows the floor plan.

In the near-field region, signal is radiated anomalistically because of the feedback to the transmitter. Therefore, the minimum distance between a transmitter and a receiver should be larger than 2 meters to avoid the near-field area effect, and the far-field area [24] γ is given as

$$\begin{cases} \gamma > \lambda, & \text{if antenna is shorter than half of the wave length} \\ \gamma > 2D^2/\lambda, & \text{else} \end{cases} \tag{4.1}$$

where λ is the wavelength and D is the largest dimension of an antenna.

The length of the 770 MHz antenna we used is 14.6 cm while the wavelength λ of 770 MHz is 38.6 cm, thus resulting in the minimum distance of 78 cm. The length of the 2.401 GHz anttenna is 15 cm and its wave length is 12.5 cm. As a result, the far-field area starts from 36 cm. However the far-field area determined from measurements is about 1.7 meter which is larger than the theoretical ones, and

thus we have chosen 2 meters as the minimum distance between the transmitter and the receiver in our experiments.

Throughout our measurements, we use the USRP N210 ith daughter boards of XCVR 2450, WBX, and SBX. Four laptops are used as a host PC where each laptop is installed with Intel Core i7-2620M (2.7 GHz, 2 cores), 8 GB RAM, 180 GB SSD, and Ubuntu 11.10. In addition, GNU Radio vesion 3.4.2 and UHD 003.003.000 are used, and the Raw OFDM [25] was used to transmit and receive OFDM signals.

It is need to know the USRP transmission power and received signal strength to measure a WAF, FAF and path loss, however, USRP can not measure a signal strength because it is an uncalibrated device. Therefore we measured SNR instead of measuring signal strength, and connected two USRPs directly through 50 Ω cable with a 50 dB attenuator to get the USRP transmission SNR. It is recommended to use a attenuator at least 30 dB because connecting two USRPs without an attenuator would damage the devices. As a result, the USRP transmission SNR was about 27.5 dB at 770 MHz and 2.401 GHz, which means the original USRP transmission SNR was about 77.5 dB. This SNR was used for a reference SNR of transmitters in the WAF, FAF and path loss measurements.

Chapter 5

Spectrum Characteristics Comparison between TVWS and ISM

Super Wi-Fi has better penetrability than Wi-Fi thanks to its lower frequency which is particularly beneficial when there are many obstacles such as walls, doors, and partitions as in indoor environments. Therefore, it is expected that Super Wi-Fi would have wider coverage than Wi-Fi not only in outdoor environments but also in indoor environments. The degree of penetration can be measured in many ways, and WAF and FAF are two most typical metrics used in the literature. Although there have been many measurement studies regarding WAF and FAF, none of them have measured them for TVWS bands and ISM bands in the same indoor environment. In this chapter, we provide our measurement results on the two metrics for the two representative frequencies, 770 MHz and 2.401 GHz.

5.1 Wall Attenuation Factor Comparison

There are four types of walls (including doors) in the fourth floor of the EB2 building at UNIST – metal doors, thick and thin ply wood walls, and compound walls. Figure 4.2 presents the locations of the tested walls where (a) is a metal door, (b) is a thick and thinply wood wall, (c) is a compound wall. Figure 5.1 shows the pictures of the listed walls. Table 5.1 shows the specification of the walls. The compound wall consists of 97% ply wood and 3% metal.

	Thickness (cm)
Metal Door	5
Thick Wall	123
Thin Wall	18
Compound Wall	7.5

Table 5.1: Specification of walls

(a) Metal door (b) Thick/Thin ply wood wall (c) Compound wall

Figure 5.1: Picture of the walls used for measuring WAF

WAF can be determined by observing the difference in signal power measured in two cases – with and without a wall between a transmitter and a receiver. In this thesis, SNR was used as a tool for the WAF measurement assuming noise power is steady. WAF is obtained by using the Multi-Wall model [20]:

$$\overline{PL}(d)[dB] = \overline{PL}(d_0) + 10n_{MF} \cdot log(\frac{d}{d_0}) + \sum WAF[dB] \tag{5.1}$$

where $\overline{PL}(d)$ is the average path loss in dB at the distance d between the transmitter and the receiver, $\overline{PL}(d_0)$ represents the path loss at the reference distance d_0, n_{MF} denotes the measured path loss exponent through multiple floors, and WAF is the attenuation factor by each wall. As mentioned in the previous chapter, the USRP's transmission SNR is 77.5 dB. Therefore, it is easy to know the path loss $\overline{PL}(d)$ and $\overline{PL}(d_0)$ at the distance d_0 and d by measuring SNR at that distances, and we can obtain WAF by setting the reference distance d_0 as 2 meters because the distance d between the transmitter and receiver was 2 meters. As a result, WAF is obtained by difference between the path losses at the distance d and d_0, since the log term is zero.

The transmitter and receiver were in opposite of each other. The tested wall is placed in the middle of the transmitter and the receiver, and SNR is measured by moving the transmitter-receiver pair along the wall in the step of 10 cm. The set of measurements is averaged out because the wall materials may not be homogeneous. Figure 5.2 depicts the procedure of the WAF measurement.

The latitude of the transmitter and receiver antenna is set to 1.3 meter from the floor in all tests except the test for the metal door. For the metal door, the measurements have benn conducted at 0.9 meter and 1.3 meter height to examine the impact of the small window on signal penetration. WBX and XCVR2450 daughter boards are used for 770 MHz and 2.401 GHz measurements, respectively, and the

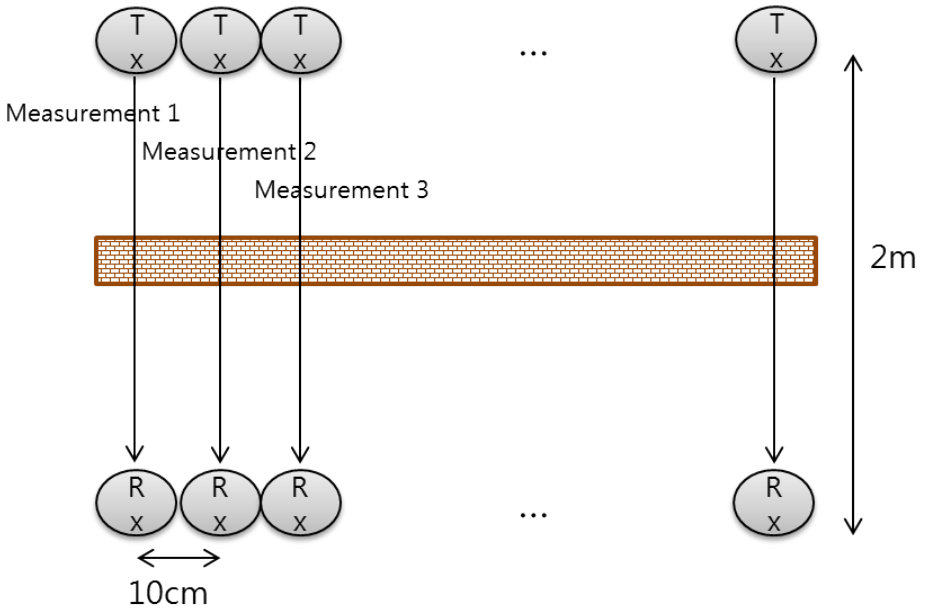

Figure 5.2: Discription of WAF measurement procedure

different gain and digital amp are set as in Table 5.2 because appropriate gain and amp depend on the daughter board as mentiond previous section 3.1.

Table 5.2: Daughter board setting

	WBX	XCVR 2450
Transmitter Gain (dB)	31	27
Receiver Gain (dB)	35	0
Digital Amplitude	0.1	0.1

Figure 5.3 shows the result of WAF measurements for the four types of walls in 770 MHz and 2.401 GHz. As shown in the graph, 770 MHz has lower WAF than Wi-Fi for the all walls, and 770 MHz penetrates the wall with very little loss. On the other hand, 2.401 GHz lose almost its power except for the wood walls and lose more power than 770 MHz about 6 times for the metal door and about 10 times for the compound wall.

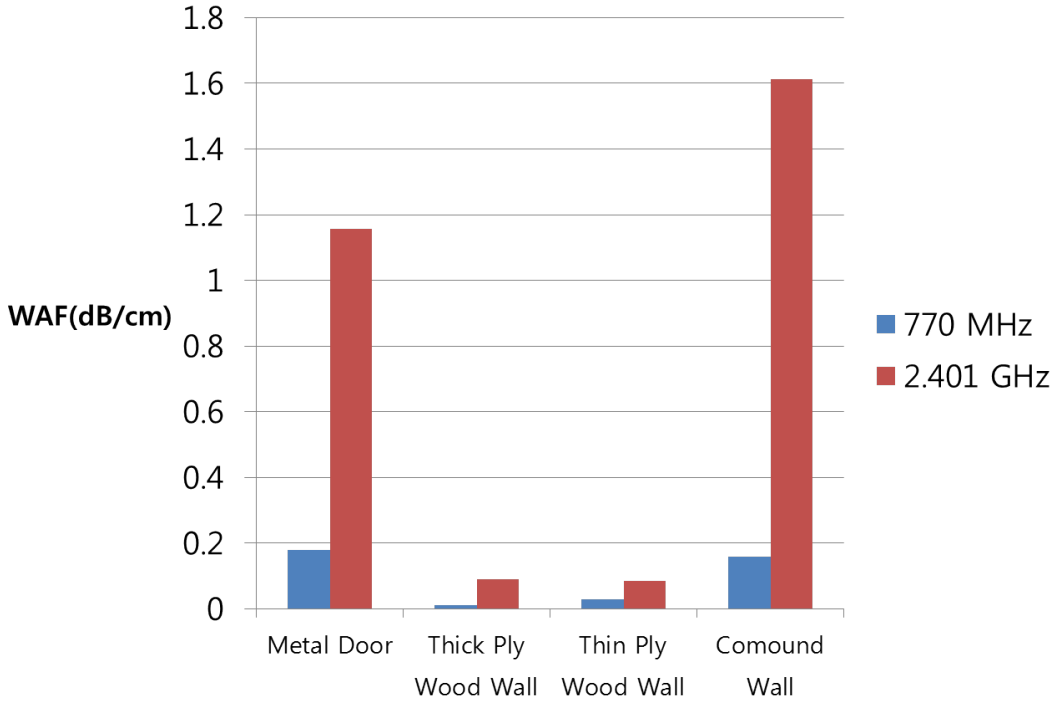

Figure 5.3: WAF measurement result

5.2 Floor Attenuation Factor Comparison

For FAF measurements, the transmitter is fixed at the fifth floor while the receiver is moving along the corridor of the third, fourth, and fifth floor up to the distance of 17 meters at the step of 30 cm. The procedure of the FAF measurement is dipicted in Figure 5.4, and the measurement locations were selected to avoid the staircases because the signals may travel along the staircase and affect the received signal strength. The transmitter and the receiver are not placed directly below to avoid the null of omnidirectional whip antenna [11]. The floor attenuation factor is defined as the difference between the average SNR of the fifth floor and the averge SNR of the third or fourth floor. Figure 5.5 shows the result that Super Wi-Fi has a smaller floor attenuation factor than Wi-Fi and can penetrates up to two floors whereas Wi-Fi can penetrate only up to a single floor. Super Wi-Fi penetrates one floor with very little signal loss with FAF of 0.635 dB, and its FAF over two floors is 9.88 dB. The Wi-Fi's attenuation factor for one floor is 12.76 dB which is even worse than the FAF Super Wi-Fi over the two floors. The result of the FAF measurement implies that Super Wi-Fi can provide reliable signal strength even when users are located at different floors.

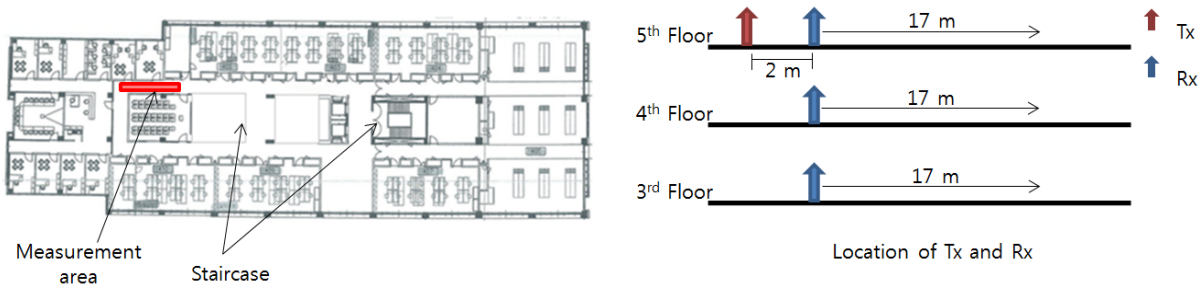

Figure 5.4: FAF measurement procedure

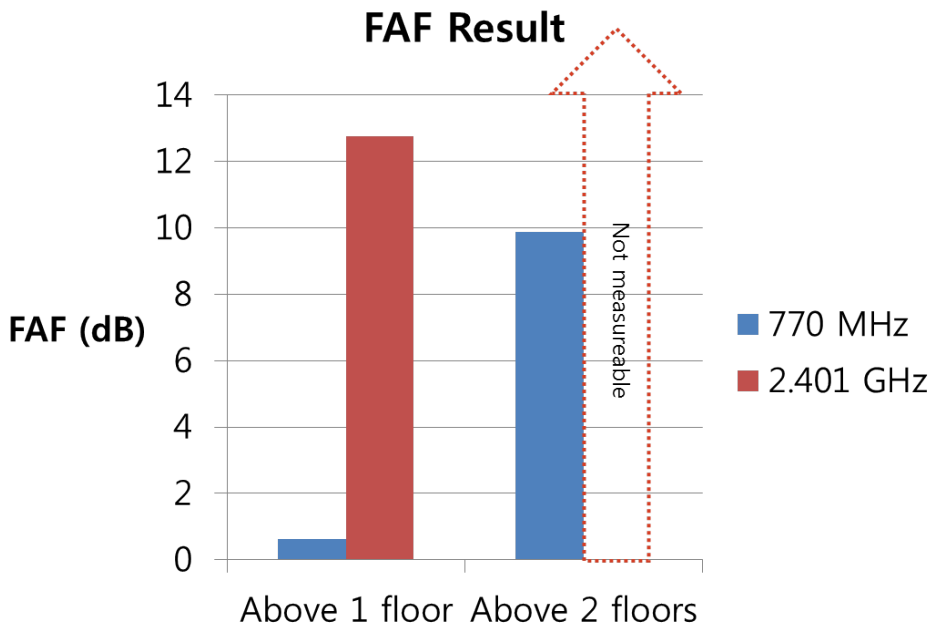

Figure 5.5: FAF comparison between Super Wi-Fi and Wi-Fi

5.3 Single-Floor Signal Propagation Measurement

The path loss measurement was conducted on the fourth floor of the EB2 building at UNIST. The transmitter is placed between elevators and a staircase, and its location is shown in Figure 4.2 (e). The receiver is moved on the fourth floor at the step of 1 meter, where the receiver locations include the whole hallways and two laboratory rooms. Although not all laboratory rooms are tested due to the limited authorization, the tested rooms well capture the propagation characteristics of Super Wi-Fi and Wi-Fi thanks to the symmetry of the building structure.

At each receiver location, SNR is measured 5 times by slightly changing each position by 10 cm in order to average out the impact of fading. To manage the same transmission power in 770 MHz and 2.401 GHz, SBX daughter board has been adopted as it can cover both 770 MHz and 2.401 GHz. The version of GNU Radio, RawOFDM, UHD, Ubuntu and laptop was the same as in the prior measurement settings, and the transmitter and receiver gain is set to 12 dB and 31 dB respectively, amp is set as 0.4, and the height of the transmitter/receiver is 1.3 meter.

Figures 5.6 and 5.7 illustrate the SNR measurement results of Super Wi-Fi and Wi-Fi. As shown, the SNR of Super Wi-Fi is better than the SNR of Wi-Fi in most measurement locations, which implies that Super Wi-Fi has a superior penetrability, diffraction, and path loss exponent than Wi-Fi. Table 5.3 is the average of the SNR measurement results.

	770 MHz (dB)	2.401 GHz (dB)
Room	17.272	6.417
Corridor	25.066	12.574
Room + Corridor	20.389	8.88

Table 5.3: Average SNR at EB2 building of the UNIST

Path loss exponent in the fourth floor of EB2 building of the UNIST was calculated by using the FAF path loss model [8]. Table 5.4 presents the categorized path loss exponent according to room and corridor. As expected, the path loss exponent in corridor is smaller (thus better) than the path loss exponent in room, thanks to the absence of obstacles and the waveguide effect.

Path Loss Exponent	770 MHz	2.401 GHz
Room	3.3345	5.1325
Corridor	2.4852	4.0947
Room + Corridor	2.684	4.2188

Table 5.4: Path loss exponent of 770 MHz and 2.401 GHz

To eliminate the effect of WAF on path loss exponent, we calculated path loss exponenets by using

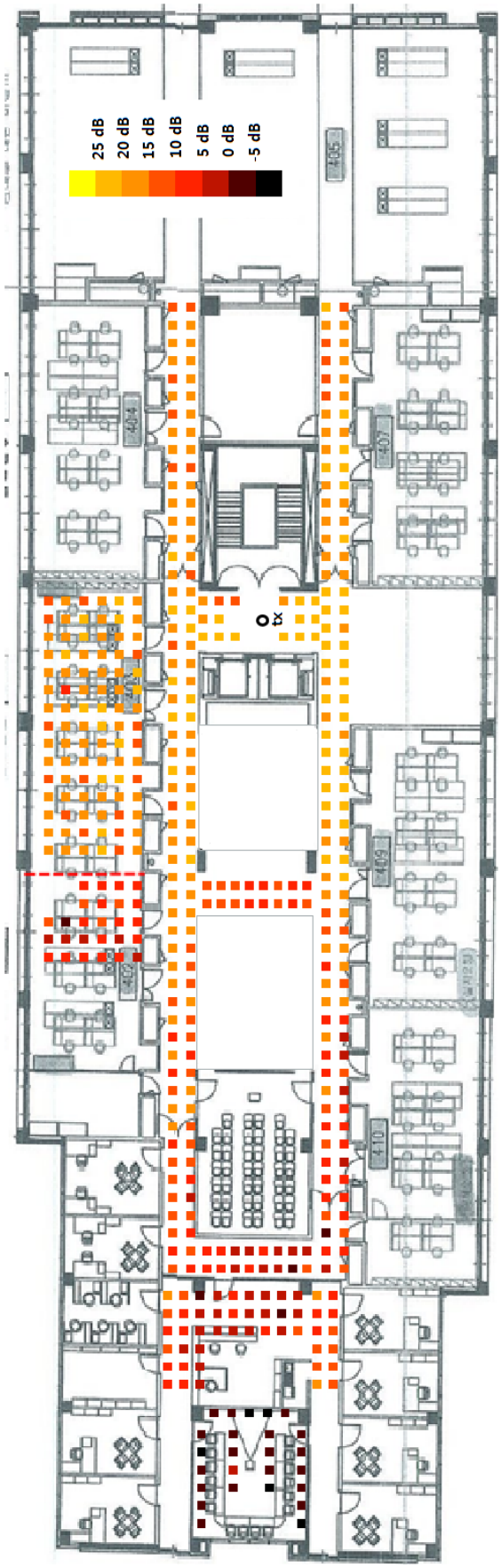

Figure 5.6: SNR measurement result at 2.401 GHz

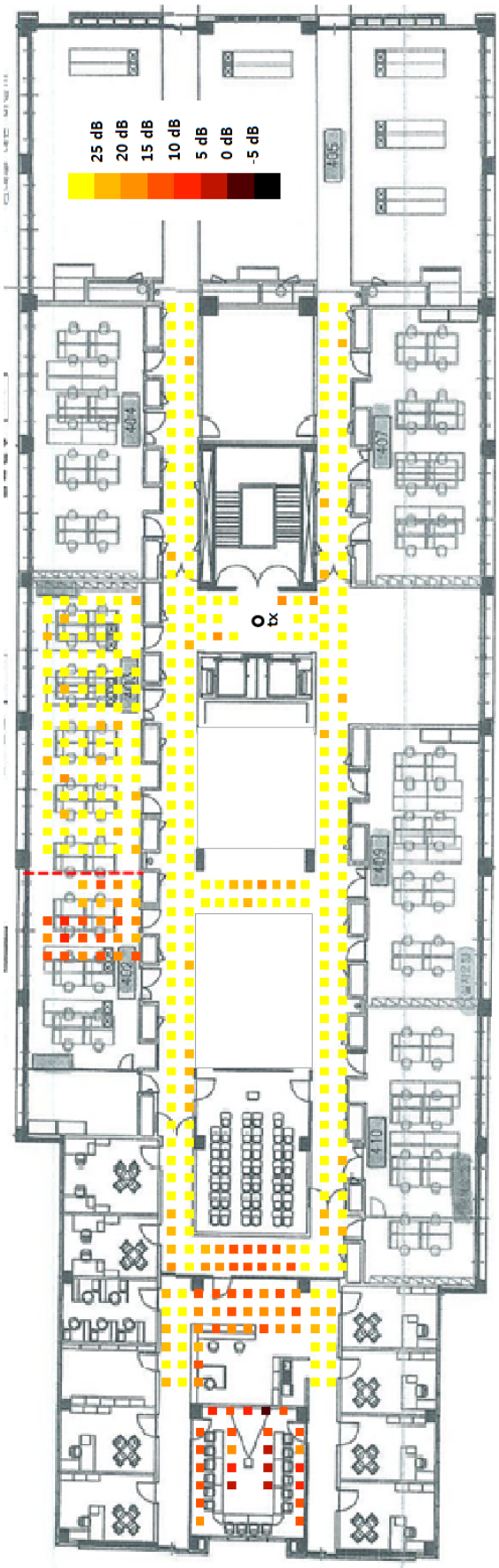

Figure 5.7: SNR measurement result at 770 MHz

WAF path loss model in Eq. (5.1) at some locations. The locations are a portion of the area between the two black lines in Figure 4.2. Such locations are affected by either metal door or thick ply wood wall. In the considered scenario, we calculated two path loss exponents, by using (1) the model in Eq. (3.2) excluding WAF where the effect of WAFs are integrated in the measured path loss exponent, and (2) the model in Eq. (5.1) that specifies the WAFs of the metal door and the thick ply wood wall. The path loss exponents from the first model are measured as 1.89 and 2.93 for 770 MHz and 2.401 GHz, respectively, and the path loss exponents from the second model are predicted as 1.79 and 2.38 for 770 MHz and 2.401 GHz, respectively. Regarding 770 MHz, the difference between the two path loss exponents from the models is only about 0.1 which is due to the small WAFs, i.e., 0.89 for the metal door and 1.95 for the thick ply wood wall. In case of 2.401 GHz, however, the difference is around 1.65 and thus much larger than in 770 MHz because of the large WAFs, i.e., 5.78 for the metal door and 11.01 for the thick ply wood wall. In addition, the path loss exponent from the first model is always larger since the measured exponent includes the additional path loss due to the walls.

5.4 Downlink Capacity

In estimating downlink capacity, we need to interprete the SNR measurements performed with 200 kHz bandwidth in to the bandwidths of interest, i.e., 6, 12, and 24 MHz for Super Wi-Fi and 20 MHz for Wi-Fi. To do so, it is critical to correctly understand how USRPs handle the gain parameter in setting its transmission power. Although the USRP documentation states that the unit of the gain is dB, it does not indicate what the reference metric is. Since Ettus Research does not provide detailed information in its internal design, we have performed an experimental study to understand its internals reference value.

In our experiment, as shown in Figure 5.8, a transmitter was placed at the center of a circle with radius 3 meters, and its receiver was rotated around the circle to measure SNR at the specified 8 positions. The receiver measured SNR 5 times at each position. The transmitter-receiver pair tested the carrier frequency of 5.52 GHz (ch 104) which has been chosen instead of 2.401 GHz because it is free of any interferers. In addition, we vary the signal bandwidth from 200 kHz to 20 MHz, while fixating the gain parameters as Tx gain of 12 and Rx gain of 31. The experiment is repeated for each chosen bandwidth, and the measurements from all 8 locations are averaged out to rule out the randomness due to fading.

Figure 5.9 illustrates the result of the measurement. We can observe, SNR stays almost constant irrelevant to bandwidth increases. This indicates that the gain parameter implies the gain in signal's power spectral density (p.s.d) measured in dB/Hz, not the signal power gain in dB. This conjecture is also verified by comparing the blue and red plots where the red plot is when the gain parameter would be regarding the power, not p.s.d. It means that the result of SNR measurement conducted with 200

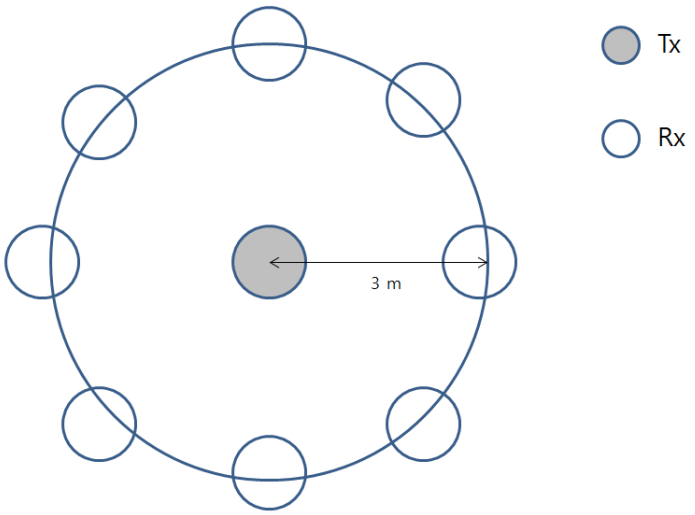

Figure 5.8: Setup for the SNR-Bandwidth measurement

kHz bandwidth can be readily used as the SNR with 6, 12, 20 or 24 MHz bandwidths as long as the

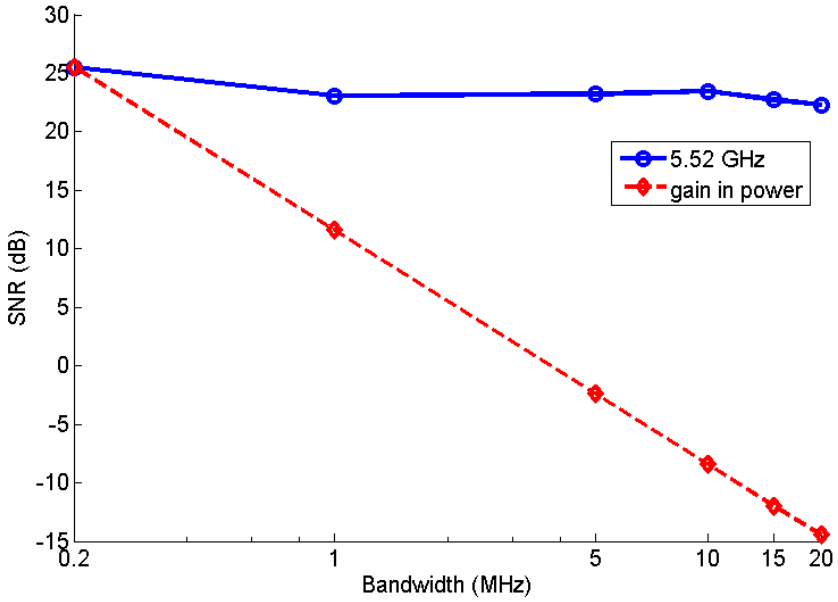

Figure 5.9: Result of the measurement to verify variation of SNR

same gain and amp values are used.

More specifically,

$$SNR = \frac{S}{N} = \frac{B \cdot 10^{(S_S+g)/10-3}}{B \cdot 10^{S_N/10-3}} = 10^{(S_S+g-S_N)/10} \tag{5.2}$$

where S and N are the power (in Watts) of signal and noise respectively, B is the signal bandwidth in Hz, S_S and S_N are the p.s.d. (in dBm/Hz) of signal (at $g = 0$) and noise respectively, g is the gain in dB/Hz. As shown, SNR only depends on the gain,and irrelevant to the bandwidth.

In this section, the channel capacity of Super Wi-Fi and Wi-Fi is estimated using the Shannon capacity:

$$C = Blog_2(1 + \frac{S}{N}) \tag{5.3}$$

where B is bandwidth in Hz; and the S and N are signal or noise power in Watt. For Super Wi-Fi, we set $B = 6$ MHz without channel bonding, and $B = 12, 24$ MHz with channel bonding. For Wi-Fi, we set $B = 20$ MHz.

Table 5.5 shows the estimation result of downlink capacity. Even though the SNR of Super Wi-Fi is better than that of Wi-Fi, the downlink capacity of Wi-Fi is heigher than the downlink capacity of Super Wi-Fi with out channel-bonding. This is because the larger bandwidth of Wi-Fi (20 MHz) than that of the Super Wi-Fi's (6 MHz). However with bonding two channels (i.e., 12 MHz), the downlink capacity of Super Wi-Fi becomes similar to the downlink capacity of Wi-Fi in a single-floored scenario. Figures

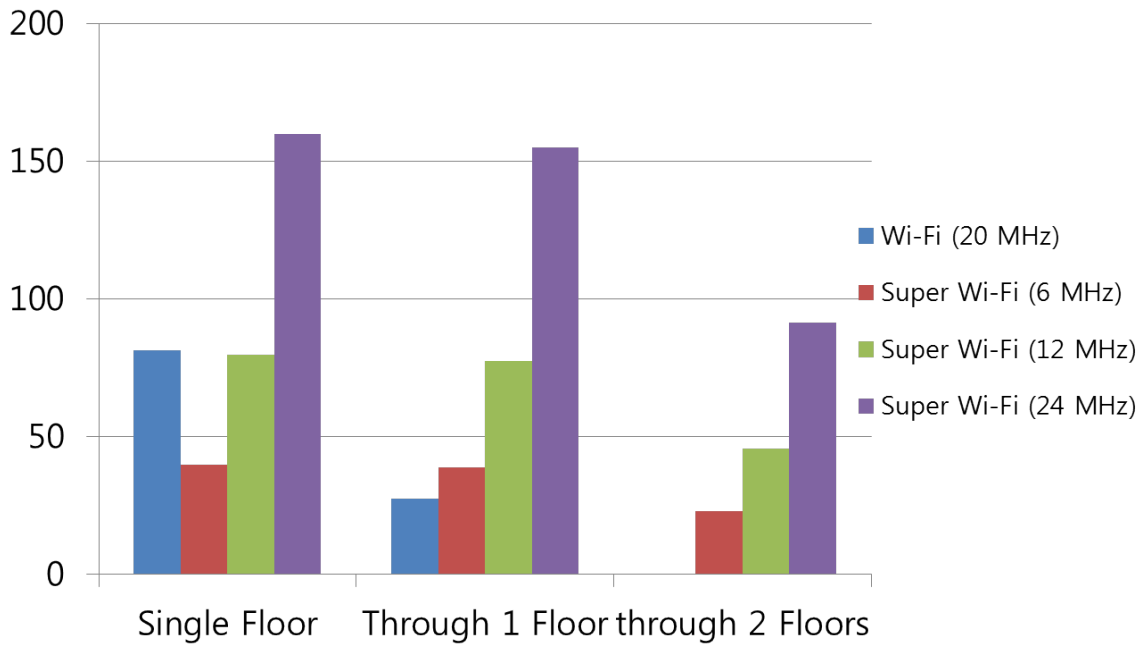

Figure 5.10: Downlink Capacity Result

5.11, 5.12, 5.13, and 5.14 present the impact of channel bonding via the following observations. First, the downlink capacity of Wi-Fi is decreased dramatically when signal travels farther than 40 meters, where the downlink capacity becomes worse than Super Wi-Fi without channel bonding. Second, Super Wi-Fi supports stable downlink capacity all over its coverage. Third, the downlink capacity of Super Wi-Fi with channel-bonding has much better downlink capacity than Wi-Fi. As a result, it is clear that Super Wi-Fi can support stable downlink capacity all over its coverage and provide stations with increased downlink capacity when Super Wi-Fi uses channel-bonding.

When signal penetrated over two floors, the downlink capaicty of Super Wi-Fi is always better than the downlink capacity of Wi-Fi. Figure 5.10 compares there downlink capacities, and 5.5 shows the specific result. We can not calculate the downlink capacity of Wi-Fi when signal penetrated two floors because the 2.401 GHz signal was not received.

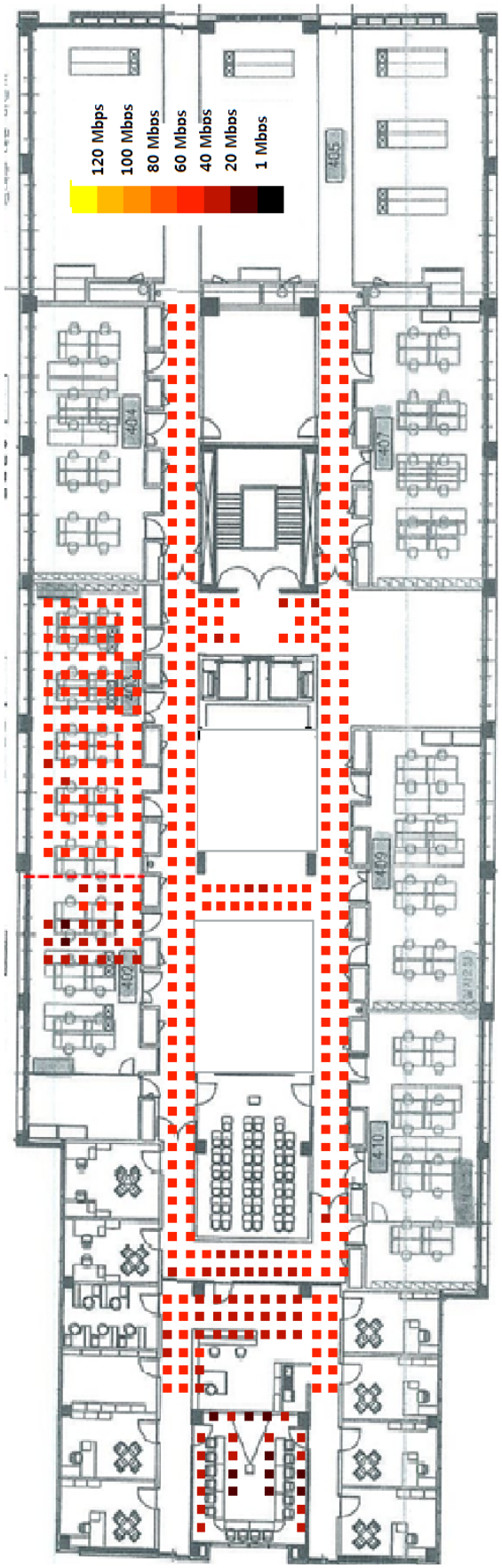

Figure 5.11: Donwlink capacity of Super Wi-Fi without channel-bonding (6 MHz) in a single-floor

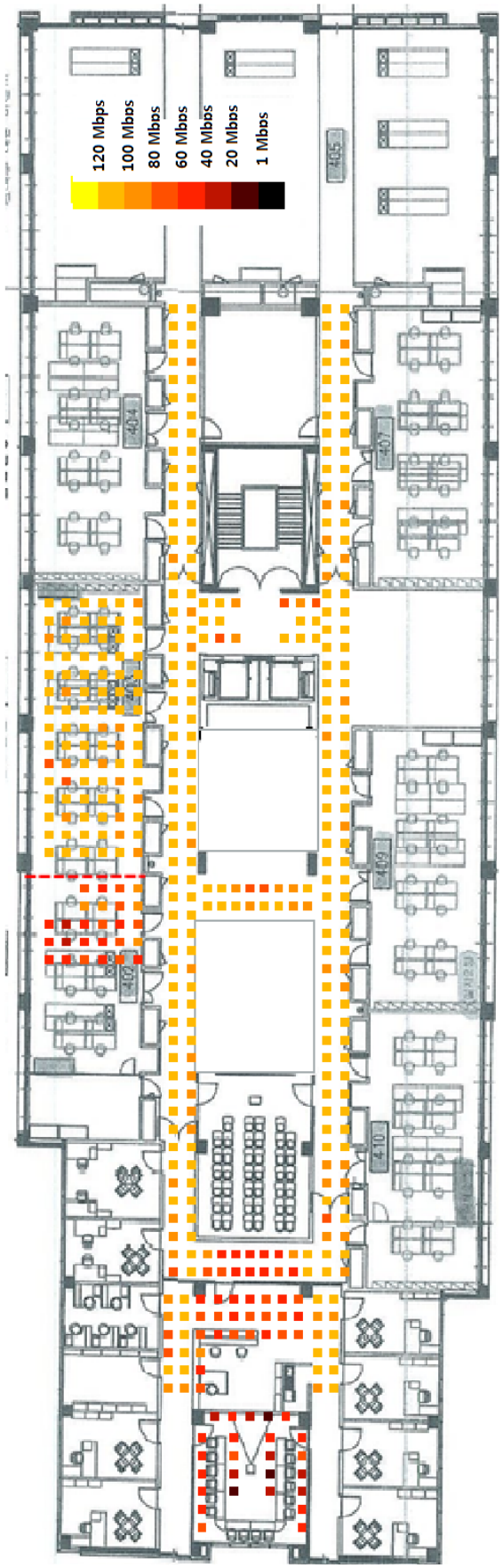

Figure 5.12: Donwlink capacity of Super Wi-Fi with 2 bonded channels (12 MHz) in a single-floor

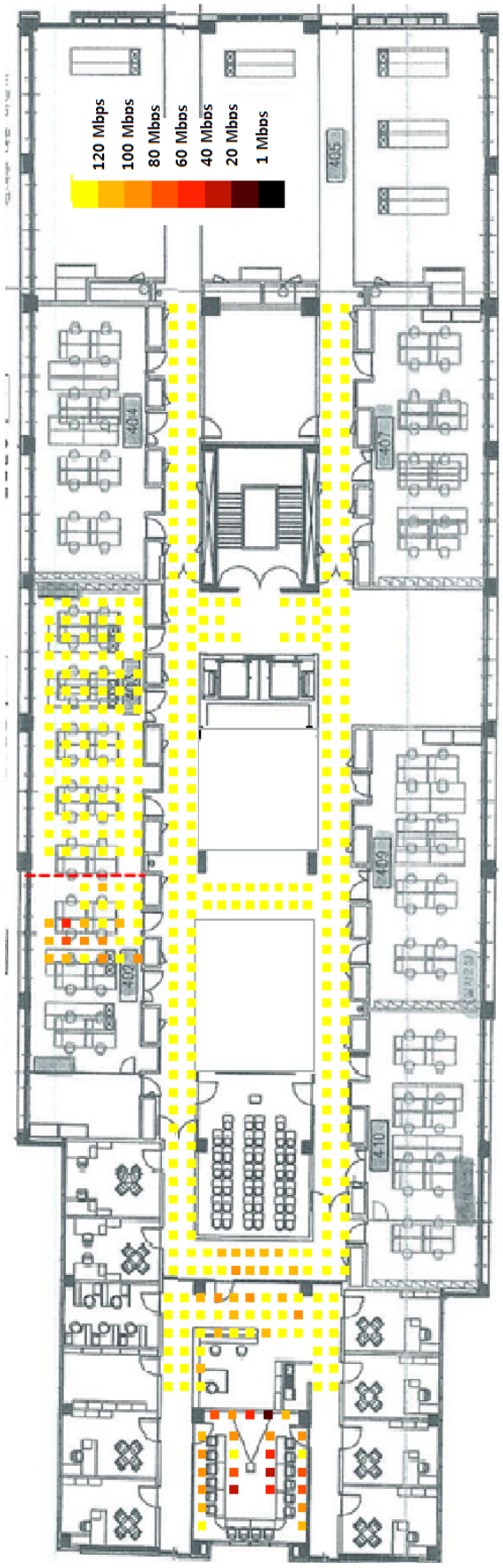

Figure 5.13: Donwlink capacity of Super Wi-Fi with 4 bonded channels (24 MHz) in a single-floor

Figure 5.14: Downlink capacity of Wi-Fi (20 MHz) in a single-floor

		Same Floor	Through 1 Floor	Through 2 Floors
Super Wi-Fi (dB) (6 MHz)	Room	34.75	33.61	18.47
	Corridor	47.71	46.52	29.43
	Room + Corridor	39.93	38.77	22.86
Super Wi-Fi (dB) (12 MHz)	Room	69.49	67.22	36.95
	Corridor	95.43	92.03	58.86
	Room + Corridor	79.87	77.55	45.71
Super Wi-Fi (dB) (24 MHz)	Room	138.99	134.45	73.89
	Corridor	190.85	186.06	117.72
	Room + Corridor	159.73	155.09	91.43
Wi-Fi (dB) (20 MHz)	Room	71.44	22.88	
	Corridor	96.66	34.34	
	Room + Corridor	81.53	27.46	

Table 5.5: Result of downlink capacity

Chapter 6

Conclusion

In this thesis, we have comapred the characteristics of Super Wi-Fi and Wi-Fi in the same indoor environments in terms of WAF, FAF and path loss. Moreover, we have estimated the downlink capacity of Super Wi-Fi and Wi-Fi indoors, based on the extensive path loss measurements. We have verified that Super Wi-Fi has superior frequency characteristics than Wi-Fi such as better wall-penetration ability and less path loss. As a result, it is expected that Super Wi-Fi provides wider coverage and more evenly-distributed data rates within its coverage than today's Wi-Fi. Without channel-bonding (6 MHz), Super Wi-Fi achieves 48.97% of Wi-Fi's downlink capacity (20 MHz) in a single-floored scenario and 141% at one floor above or below where the transmitter is located. With two bonded channels (12 MHz), Super Wi-Fi achieves 97% of Wi-Fi's downlink capacity in a single-floored scenario and 282% at one floor above or below scenario. Moreover, Super Wi-Fi with four bonded channels (24 MHz) achieves 195% of Wi-Fi's downlink capacity in a single floored environment and 564% at one floor above or below environments. These results show that Super Wi-Fi has potential to become a successful application in indoor environments.

It has been shown that Super Wi-Fi has the superior characteristics and can provide large enough downlink capacity for indoor applications. By utilizing these advantages, new scenarios like coexisting Wi-Fi with Super Wi-Fi can be considered as future direction of Super Wi-Fi research. Moreover, deciding when is the best case to replace Wi-Fi with Super Wi-Fi in a single-floored environment is of great interest, since it can improve not only the performance of Wi-Fi but also Super Wi-Fi's performance. In addition, it will be possible to predict whether it is useful to use Super Wi-Fi or not in given indoor environment by developing a prediction mechanism.

REFERENCE

[1] Microsoft. Microsoft Spectrum Observatory. http://spectrum-observatory.cloudapp.net

[2] HYOIL KIM, K. S. A. C. J. 2013. Downlink Capacity of Super Wi-Fi Coexisting with Conventional Wi-Fi. IEEE Global Communications Conference

[3] JOSHI, T., MUKHERJEE, A., YOO, Y. & AGRAWAL, D. P. 2008. Airtime fairness for IEEE 802.11 multirate networks. Mobile Computing, IEEE Transactions on, 7, 513-527

[4] ANDERSEN, J. B., RAPPAPORT, T. S. & YOSHIDA, S. 1995. Propagation measurements and models for wireless communications channels. Communications Magazine, IEEE, 33, 42-49.

[5] HONCHARENKO, W., BERTONI, H. L., DAILING, J. L., QIAN, J. & YEE, H. 1992. Mechanisms governing UHF propagation on single floors in modern office buildings. Vehicular Technology, IEEE Transactions on, 41, 496-504.

[6] LAFORTUNE, J.-F & LECOURS, M. 1990 Measurement and modeling of propagation losses in a building at 900 mhz. IEEE Trans. Veh. Technol. 39, 101–108.

[7] PORRAT, D. & COX, D. C. 2004. UHF propagation in indoor hallways. Wireless Communications, IEEE Transactions on, 3, 1188-1198.

[8] SEIDEL, S. Y. & RAPPAPORT, T. S. 1992. 914 MHz path loss prediction models for indoor wireless communications in multifloored buildings. Antennas and Propagation, IEEE Transactions on, 40, 207-217.

[9] ZVANOVEC, S., PECHAC, P. & KLEPAL, M. 2003. Wireless LAN networks design: site survey or propagation modeling? Radioengineering, 12, 42-49.

[10] ANDERSON, C. R. & RAPPAPORT, T. S. 2004. In-building wideband partition loss measurements at 2.5 and 60 GHz. Wireless Communications, IEEE Transactions on, 3, 922-928.

[11] ANDRUSENKO, J., MILLER, R. L., ABRAHAMSON, J. A., MERHEB EMANUELLI, N. M., PATTAY, R. S. & SHUFORD, R. M. 2008. VHF general urban path loss model for short range ground-to-ground communications. Antennas and Propagation, IEEE Transactions on, 56, 3302-3310.

[12] GAIEWSKI, P., SUCHAKISKI, P. K. & MATYSZKIEL, R. 2011. Prediction of VHF Radio Wave Attenuation in an Urban Environmentl.

[13] TAYLOR, C. D., GUTIERREZ, S. J., LANGDON, S. L., MURPHY, K. L. & WALTON III, W. A. 1997. Measurement of RF Propagation into Concrete Structures over the Frequency Range 100 MHZ to 3 GHz. Wireless Personal Communications. Springer.

[14] PENA, D., FEICK, R., HRISTOV, H. D. & GROTE, W. 2003. Measurement and modeling of propagation losses in brick and concrete walls for the 900-MHz band. Antennas and Propagation, IEEE Transactions on, 51, 31-39.

[15] SIMIC, L., PETROVA, M. & MAHONEN, P. Wi-Fi, but not on steroids: Performance analysis of a Wi-Fi-like network operating in TVWS under realistic conditions. Communications (ICC),

2012 IEEE International Conference on, 2012. IEEE, 1533-1538.

[16] Ettus Research, Universal Software Radio Peripheral, http://ettus.com/

[17] GNU Radio, http://gnuradio.org/redmine/projects/gnuradio/wiki

[18] HATA, M. 1980. Empirical formula for propagation loss in land mobile radio services. Vehicular Technology, IEEE Transactions on, 29, 317-325.

[19] COST. 1991. Urban Transmission Loss Models for Mobile Radio in the 900- and 1,800 MHz Bands: (revision 2), COST 231.

[20] RAPPAPORT, T. S. 1996. Wireless communications: principles and practice, Prentice Hall PTR New Jersey.

[21] ACTION, C. 1999. Digital Mobile Radio Towards Future Generation Systems: Final Report, Directorate General Telecommunications, Information Society, Information Market, and Exploitation Research.

[22] RECOMMENDATIONS, I. 2001. Propagation data and prediction methods for the planning of indoor radio communication systems and radio local area networks in the frequency range 900MHz to 100GHz. ITU Recommendations.

[23] SUNGWOONG CHOI, S. C et al. 2011. Technology standard trends for utilization in tv white space. Electronics and Telecommunications Trends 26, 68–78.

[24] SUCHANSKI, M., KANIEWSKI, P., MATYSZKIEL, R. & GAJEWSKI, P. Prediction of VHF and UHF wave attenuation in urban environment. Microwave Radar and Wireless Communications (MIKON), 2012 19th International Conference on, 2012. IEEE, 60-65.

[25] Jakubczak, S. K. 2010. RawOFDM, http://people.csail.mit.edu/szym/rawofdm/README.html

Acknowledgement

I would like to thank Prof. Hyoil Kim, Changhee Joo, Hyun Jong Yang and all members of WMNL.